High-Spin Molecules: Iron(III) Incorporation into $[Mn_{12}O_{12}(O_2CMe)_{16}(H_2O)_4]$ To Yield $[Mn_8Fe_4O_{12}(O_2CMe)_{16}(H_2O)_4]$ and Its Influence on the $S = 10$ Ground State of the Former

Ann R. Schake,[1a] Hui-Lien Tsai,[1b] Robert J. Webb,[1b] Kirsten Folting,[1c] George Christou,*[1a] and David N. Hendrickson*[1b]

Department of Chemistry and Molecular Structure Center, Indiana University, Bloomington, Indiana 47405, and Department of Chemistry-0358, University of California at San Diego, La Jolla, California 92093-0358

Received May 6, 1994[⊗]

The synthesis, single-crystal X-ray structure, and electrochemical, magnetochemical and Mössbauer properties are reported for $[Mn_8Fe_4O_{12}(O_2CMe)_{16}(H_2O)_4]$ (**3**) as its $2MeCO_2H{\cdot}4H_2O$ solvate. Complex **3** represents the partially Fe^{III}-substituted form of $[Mn_{12}O_{12}(O_2CMe)_{16}(H_2O)_4]$ (**1**), for which the benzoate analogue, $[Mn_{12}O_{12}(O_2CPh)_{16}(H_2O)_4]$ (**2**) is also known. Treatment of $Fe(O_2CMe)_2$ with $KMnO_4$ (16.3:6.4 molar ratio) in 60% aqueous acetic acid followed by slow heating to 60 °C, cooling to room temperature and layering of the golden brown solution with acetone, leads to black crystals of $3{\cdot}2MeCO_2H{\cdot}4H_2O$ in ~85% yield. The crystals are isomorphous with $1{\cdot}2MeCO_2H{\cdot}4H_2O$, with the following unit cell parameters at −158 °C: tetragonal, $I\bar{4}$, $a = b = 17.169(4)$, $c = 12.258(3)$, $V = 3612.9$ Å^3 and $Z = 2$. The structure was solved (MULTAN) and refined employing 3211 unique reflections with $F > 3\sigma(F)$ to final values of $R = 0.0768$ and $R_w = 0.0768$. The molecule consists of a central $[Mn^{IV}_4O_4]^{8+}$ cubane held within a nonplanar ring of eight alternating Mn^{III} and Fe^{III} ions by eight μ_3-O^{2-} ions. Peripheral ligation is provided by sixteen μ-$MeCO_2^-$ and four terminal H_2O groups, the latter being ligated one each on the four Fe^{III} ions. The identification of the Fe^{III} ions was facilitated by the absence of a Jahn-Teller axial elongation as seen for the Mn^{III} ions. Elemental analysis data suggest a small fraction of molecules contain Fe^{III} ions at the Mn^{III} sites; Fe:Mn analysis ratios are approximately 4.37:7.63. Electrochemical studies in MeCN solution using cyclic voltammetry reveal a quasireversible oxidation at 0.81 V vs ferrocene and a quasireversible reduction at 0.17 V, in addition to irreversible oxidation and reduction features. The reversible processes occur at essentially identical potentials as for **1** suggesting the reduction and oxidation processes are occurring at manganese centers. ^{57}Fe Mössbauer spectra are reported for $3{\cdot}2MeCO_2H{\cdot}4H_2O$ at 300 and 120 K. At both temperatures there are two doublets present. A fit of the 300 K spectrum shows that the area associated with the main doublet is 82.6% of the total. This doublet has a quadrupole splitting (ΔE_Q) of 0.459(4) mm/s and is attributable to the four high-spin Fe^{III} ions identified in the X-ray structure. The other doublet with $\Delta E_Q = 1.061(2)$ mm/s at 300 K is assignable to the excess high-spin Fe^{III} which is disordered throughout the Mn^{III} sites. For a polycrystalline sample of $3{\cdot}2MeCO_2H{\cdot}4H_2O$ embedded in parafilm in a 10.0 kG field the value of μ_{eff} per molecule is 11.18 μ_B at 300.0 K and decreases gradually with decreasing temperature to 4.85 μ_B at 5.00 K. Least-squares fitting of 0.50-50.0 kG data in the 2.0-30 K range with a full matrix diagonalization approach shows that this Fe_4Mn_8 complex has a well-isolated $S = 2$ ground state with an axial zero-field splitting of $D = -1.8$ cm^{-1}. The origin of the change from a $S = 10$ ground state for the $Mn^{IV}_4Mn^{III}_8$ complex **1** to a $S = 2$ ground state for $Mn^{IV}_4Mn^{III}_4Fe^{III}_4$ complex **3** is discussed.

Introduction

The preparation of molecules with large numbers of unpaired electrons represents an area of considerable current interest. It is widely recognized that such molecules are attractive as potential building blocks for molecular-based magnetic materials.[2] A number of strategies are currently available to access the latter. One family of organometallic ferromagnets employs salt formation between metallocene cations (D^+) and organic anions (A^-), each with an unpaired electron ($S = {}^1/_2$), arranged in alternating stacks.[3] Pairwise ($D^{+}\cdots A^{-}$) magnetic exchange interactions in each stack are important, as are the interactions between stacks, for it is the latter that dictate the overall ferromagnetic ordering at low temperatures. A second strategy involves the formation of ferrimagnetic chains consisting of bridged heterometallic (Cu^{II}-L-Mn^{II}) (L = a bridging organic group) building blocks.[4] Again, the relative alignment (registry) of the chains is crucial, for it controls interchain magnetic exchange interactions and the likelihood of net ferromagnetic coupling between chains. A third strategy that has yielded molecular ferromagnets involves covalently-linked heterospin chains as before, but now one of the alternating species possessing unpaired electrons is an organic group.[5] Thus, chains consisting of alternating metal ions and nitroxide ($S = {}^1/_2$) groups have been prepared and found to exhibit ferromagnetism.

⊗ Abstract published in *Advance ACS Abstracts,* November 1, 1994.

(1) (a) Department of Chemistry, Indiana University. (b) University of California, at San Diego. (c) Molecular Structure Center, Indiana University.

(2) (a) *Magnetic Molecular Materials*; Gatteschi, D., Kahn, O., Miller, J. S., Palacio, F., Eds.; NATO ASI Series E, 198; Kluwer Academic Publishers: Dordrecht, The Netherlands, 1991. (b) Kahn, O.; Pei, Y.; Journaux, Y. Molecular Inorganic Magnetic Materials In *Inorganic Materials*; Bruce, D. W., O'Hare, D., Eds.; Wiley & Sons Ltd.: New York, 1992; pp 59-114.

(3) (a) Miller, J. S.; Epstein, A. J.; Reiff, W. M. *Chem. Rev.* **1988**, *88*, 201. (b) Miller, J. S.; Epstein, A. J.; Reiff, W. M. *Acc. Chem. Res.* **1988**, *21*, 114.

(4) (a) Kahn, O. *Struct. Bonding (Berlin)* **1987**, *68*, 89. (b) Kahn, O.; Pei, Y.; Nakatani, K.; Journaux, Y. *Mol. Cryst. Liquid Cryst.* **1989**, *176*, 481.

(5) Caneschi, A.; Gatteschi, D.; Sessoli, R. *Acc. Chem. Res.* **1989**, *22*, 392.

0020-1669/94/1333-6020$04.50/0

It is clear that the types of studies described above establish the feasibility of molecular ferromagnetism, and the challenge for the future is thus to extend these and related approaches to other molecules possessing unpaired electrons. Specifically, it is important to access new and various molecular species with large spin values in the ground state, and to develop the manipulative methodology to link these species in an appropriate manner so as to allow long-range ferro- and/or ferrimagnetic ordering in three dimensions.

The search for molecules with large numbers of unpaired electrons is being pursued in both the organic and inorganic areas. Conjugated π organic molecules possessing several unpaired electrons have been prepared.[6] A hydrocarbon consisting of five carbene linkages and $S = 6$ has the highest spin value for an organic molecule.[7] High-spin organic structures possessing more localized bonding than that found in the conjugated π-radicals are also under investigation.[8] In the inorganic area, several high-spin molecules have been prepared such as an $[Mn^{II}_6(\text{nitroxide})_6]$ complex that has a $S = 12$ ground state,[9a] and $(Me_4N)[Mn_{10}(\text{biphen})_4O_4Cl_{12}]$ which has been reported[9b] to have a $S = 14$ ground state. Similarly, $[Mn_{12}O_{12}(O_2CMe)_{16}(H_2O)_4]$ (**1**) has a $S = 10$ ground state in zero field, and $[Mn_{12}O_{12}(O_2CPh)_{16}(H_2O)_4]$ (**2**) has a $S = 10$ or $S = 9$ ground state in a ≥ 20 kG field depending on whether the complex has no (**2**) or some ($2{\cdot}PhCO_2H{\cdot}CH_2Cl_2$) interstitial molecules in the crystal lattice.[10] In zero applied field, complex **2** has a $S = 9$ ground state.[11] Most interestingly, complexes **1** and **2** are the only molecular species known to exhibit a non-zero, out-of-phase (imaginary) component in their AC susceptibility response in zero applied field.[10] Thus, this family of metal complexes warrants additional and detailed study.

The present work derives from a desire to determine to what extent the spin of the ground state of complexes **1** or **2** would be affected by changes in the electron count of the system. One potential way of tackling this question is to oxidize or reduce the complexes; another is to substitute some of the Mn^{III} (d^4) ions with, for example, Fe^{III} (d^5) ions to give $[Mn_{12-x}Fe_xO_{12}(O_2CR)_{16}(H_2O)_4]$, thereby increasing the electron count by x electrons. Initial success along both these directions was recently communicated.[12] Herein we describe in detail the synthesis of $[Mn_8Fe_4O_{12}(O_2CMe)_{16}(H_2O)_4]$ (**3**) and an assessment of the influence of the four extra electrons on the spin of the ground state of the molecule.

Experimental Section

Compound Preparation. All chemicals and solvents were used as received; all preparations and manipulations were performed under aerobic conditions. Anhydrous iron(II) acetate (Mallinckrodt) was stored and weighed out in an inert atmosphere glovebox.

$[Mn_8Fe_4O_{12}(O_2CMe)_{16}(H_2O)_4]$ (3). Solid $KMnO_4$ (1.0 g, 6.4 mmol) was slowly added in small portions to a stirred slurry of $Fe(O_2CMe)_2$ (2.84 g, 16.3 mmol) in 60% (v/v) $MeCO_2H/H_2O$. All solids slowly dissolved to yield a deep golden-brown solution. This was slowly heated to 60 °C, allowed to cool back to room temperature, and the cooled solution layered with an equal volume of acetone. After several days, when the crystallization was judged complete, the resulting black crystals were collected by filtration, washed with acetone and dried briefly under vacuum. The yield was typically 85%, calculated on the basis of available manganese. Selected IR data (cm^{-1}): 3605 (m), 3100 (br), 1712 (m), 1588 (s), 1560 (s), 1532 (s), 1085 (s), 672 (m), 664 (m), 640 (s), 610 (m), 565 (m), 538 (m). Electronic spectrum in MeCN: λ_{max}, nm (ϵ_m, L mol^{-1} cm^{-1}); 254 (81,000), 496 (sh, 5100), 714 (900). The elemental analysis results are given below for the products from three separate preparations, showing the indicated Mn:Fe ratio. (a) Calcd (found) for $C_{36}H_{72}O_{56}Fe_{4.51}Mn_{7.49}$: C, 20.95 (21.0); H, 3.52 (3.4); Fe, 12.20 (12.05); Mn, 19.93 (19.7). (b) Calcd (found) for $C_{36}H_{72}O_{56}Fe_{4.23}Mn_{7.77}$: C, 20.95 (21.4); H, 3.52 (3.5); Fe, 11.44 (11.1); Mn, 20.68 (20.1). (c) Calcd (found) for $C_{36}H_{72}O_{56}Fe_{4.36}Mn_{7.65}$: C, 20.94 (20.6); H, 3.51 (3.4); Fe, 11.79 (11.4); Mn, 20.35 (19.6).

Table 1. Crystallographic Data for Complex $3{\cdot}2MeCO_2H{\cdot}4H_2O$

chem formula[a]	$C_{36}H_{72}O_{56}Fe_4Mn_8$	fw	2063.82
a, Å	17.169(4)	space group	$I\bar{4}$
b, Å	17.169(4)	λ(Mo, Kα), Å[b]	0.710 69
c, Å	12.258(3)	ϱ_{calc}, g/cm^{-3}	1.897
V, Å^3	3612.9	μ, cm^{-1}	21.803
Z	2	R[c]	0.0768
T, °C	−158	R_w[d]	0.0768

[a] Including solvate molecules. [b] Graphite monochromator. [c] $R = \sum||F_o| - |F_c||/\sum|F_o|$. [d] $R_w = [\sum w(|F_o| - |F_c|)^2/\sum wF_o^2]^{1/2}$, where $w = 1/\sigma^2(|F_o|)$.

X-ray Crystallography and Structure Solution. A suitable small crystal was selected from the bulk sample and transferred to the goniostat of a Picker four-circle diffractometer where it was cooled to −158 °C for characterization and data collection. A systematic search of a limited hemisphere of reciprocal space yielded a set of reflections which exhibited tetragonal ($\bar{4}$) symmetry. The systematic extinction of hkl for $h + k + l = 2n + 1$ as well as the extinction of $hk0$ for $h + k = 2n + 1$ and of $00l$ for $l = 2n + 1$ limited the choice of space groups to $I\bar{4}$, $I4$ or $I4/m$. The choice of the noncentrosymmetric space group $I\bar{4}$ was confirmed by the subsequent successful refinement of the structure. This choice was initially based on the fact that the crystal structure appeared to be isomorphous with the structure of $[Mn_{12}O_{12}(O_2CMe)_{16}(H_2O)_4]{\cdot}2MeCO_2H{\cdot}4H_2O$ (**1**). Unit cell dimensions were determined using 40 unique reflections having $24° < 2\theta < 41°$; a total of 3605 reflections were measured (including standard reflections). Following the usual data reduction and averaging of equivalent reflections (Friedel pairs were *not* averaged) a unique set of 3211 reflections was obtained. A correction for absorption was carried out. A final set of 2506 reflections was considered observed by the criterion $F > 3.0\sigma(F)$. A plot of the intensities of the standard reflections with time showed no significant fluctuations. The structure was readily solved by a standard combination of direct methods (MULTAN) and Fourier techniques. The structures of **1** and **3** are isomorphous; the identity of the Fe atom was selected from an inspection of the metal−oxygen distances. In the present structure determination, only three peaks could be clearly identified for the interstitial acetic acid molecule, namely, C(9), O(14) and O(15); refinement of the occupancies of these atoms converged at 0.5. Almost all of the hydrogen atoms except those on the coordinated H_2O as well as the interstitial H_2O were located. The full matrix least-squares refinement was completed using anisotropic thermal parameters on all non-hydrogen atoms and fixed idealized hydrogen atoms on the methyl groups. The final difference Fourier map was essentially featureless, except for a couple of peaks near the metal atoms, and near the acetic acid molecule. Final values of the discrepancy indices R and R_w are given in Table 1.

Physical Measurements. DC magnetic susceptibility measurements were carried out on a Quantum Design MPMS SQUID susceptometer equipped with a 5.5 T magnet and operating in the range of 1.7−400 K. Pascal's constants were used to estimate the diamagnetic correction for the complex, which was subtracted from the experimental susceptibility to give the molar paramagnetic susceptibility. The computer

(6) (a) Iwamura, H. *Pure Appl. Chem.* **1987**, *59*, 1595. (b) Iwamura, H. *Pure Appl. Chem.* **1986**, *58*, 187. (c) Itoh, K.; Takui, T.; Teki, Y.; Kinoshita, J. *J. Mol. Elect.* **1988**, *4*, 181.
(7) Nakamura, N.; Inoue, K.; Iwamura, H.; Fujioka, T.; *et al. J. Am. Chem. Soc.* **1992**, *114*, 1484.
(8) Dougherty, D. A. *Pure Appl. Chem.* **1990**, *62*, 519.
(9) (a) Caneschi, A.; Gatteschi, D.; Laugier, J.; Rey, P.; Sessoli, R.; Zanchini, C. *J. Am. Chem. Soc.* **1988**, *110*, 2795. (b) Goldberg, D. P.; Caneschi, A.; Lippard, S. J. *J. Am. Chem. Soc.* **1993**, *115*, 9299.
(10) Sessoli, R.; Tsai, H.-L.; Schake, A. R.; Wang, S.; Vincent, J. B.; Folting, K.; Gatteschi, D.; Christou, G.; Hendrickson, D. N. *J. Am. Chem. Soc.* **1993**, *115*, 1804.
(11) Caneschi, A.; Gatteschi, D.; Sessoli, R.; Barra, A. L.; Brunel, L. C.; Guillot, M. *J. Am. Chem. Soc.* **1991**, *113*, 5873.
(12) Schake, A. R.; Tsai, H.-L.; De Vries, N.; Webb, R. J.; Folting, K.; Hendrickson, D. N.; Christou, G. *J. Chem. Soc., Chem. Commun.* **1992**, 181.

Table 2. Atomic Coordinates ($\times 10^4$) and Isotropic Thermal Parameters (Å^2) for $[Mn_8Fe_4O_{12}(O_2CMe)_{16}(H_2O)_4]\cdot 2MeCO_2H\cdot 4H_2O$

atom	x	y	z	B_{iso}[a]
Mn(1)	4163(1)	−178(1)	1722(2)	11
Mn(2)	2575(1)	−467(1)	1662(2)	12
Fe(3)	3562(1)	−1978(1)	2716(2)	14
O(1)	4286(5)	−147(5)	3248(7)	12
O(2)	3503(5)	−1047(5)	1825(7)	12
O(3)	3250(5)	393(5)	1816(7)	11
O(4)	4141(6)	−199(6)	145(7)	15
O(5)	2882(6)	−478(6)	−102(8)	17
O(6)	2375(7)	−509(7)	3460(9)	30
O(7)	3075(6)	−1487(6)	4066(8)	21
O(8)	1641(6)	169(6)	1473(8)	16
O(9)	3594(6)	−2989(6)	3566(8)	18
O(10)	1896(6)	−1359(6)	1382(8)	21
O(11)	2482(6)	−2345(6)	2267(9)	23
O(12)	3917(6)	−2649(7)	1375(8)	23
O(13)	3127(7)	−2181(8)	−444(9)	33
O(14)	862(42)	825(41)	3712(47)	129
O(15)	561(28)	−508(38)	3548(37)	97
C(1)	3543(8)	−366(7)	−410(11)	13
C(2)	3719(9)	−487(10)	−1634(12)	26
C(3)	2736(9)	−866(10)	4159(12)	22
C(4)	2719(14)	−546(21)	−4655(15)	77
C(5)	1506(7)	875(8)	1333(10)	10
C(6)	713(9)	1086(9)	989(15)	25
C(7)	1920(7)	−2058(7)	1711(12)	13
C(8)	1271(10)	−2570(10)	1426(12)	25
C(9)	362(46)	142(69)	3757(74)	120

[a] Isotropic values for those atoms refined anisotropically are calculated using the formula given by: Hamilton, W. C. *Acta Crystallogr.* **1959**, *12*, 609.

program GENSPIN[13] was used to analyze variable-field magnetization data. The spin of the ground state is set at some value, and then the spin Hamiltonian matrix is diagonalized at each magnetic field to fit the experimental data.

Electrochemical studies were performed by using an IBM Model EC 225 voltammetric analyzer, a PAR Model 175 universal programmer, and a standard three-electrode assembly (glass-carbon working, Pt-wire auxiliary, SCE reference) with 0.1 M $NBu^n_4PF_6$ as supporting electrolyte. No *IR* compensation was employed. Quoted potential values are *vs* the ferrocene/ferrocenium couple under the same conditions. The scan rate was set at 100 mV/s. The solvent used was distilled and the concentration of the complex was 1 mM.

Variable-temperature ^{57}Fe Mössbauer spectra were obtained using a constant acceleration vertical drive spectrometer described elsewhere.[14] The temperature was controlled using a Lake Shore Cryogenics Model DRC80C temperature controller in conjunction with a Si diode mounted on the copper sample holder. The absolute accuracy is estimated at ±3 K. The spectra were fit to Lorentzian line shapes using a modified version of a previously reported computer program.[15] Isomer shift values are reported relative to Fe foil at 300 K and have not been corrected for the temperature-dependent second-order Doppler shift.

Results

The reaction between $Fe(O_2CMe)_2$ and $KMnO_4$ in 60% aqueous acetic acid leads to formation of $[Mn_8Fe_4O_{12}(O_2CMe)_{16}(H_2O)_4]$ (**3**) which can be isolated as $\mathbf{3}\cdot 2MeCO_2H\cdot 4H_2O$ in ~85% yield (based on Mn). The single-crystal X-ray structure of $\mathbf{3}\cdot 2MeCO_2H\cdot 4H_2O$ has been determined at −158 °C. Crystallographic data, atomic coordinates, and selected structural parameters are given in Tables 1−4; a labeled figure is provided in Figure 1. Electrochemical studies on **3** have been performed using cyclic voltammetry (CV) and differential pulse voltammetry (DPV). The observed scans are shown in Figure 2.

Table 3. Selected[a] Interatomic Distances and Angles (Å, deg) for $[Mn_8Fe_4O_{12}(O_2CMe)_{16}(H_2O)_4]\cdot 2MeCO_2H\cdot 4H_2O$

(a) Distances

Mn(1)−Mn(1′)	2.820(4)	Mn(1)−O(1)	1.883(10)
Mn(1)−Mn(1″)	2.938(4)	Mn(1)−O(1′)	1.924(9)
Mn(1)−Mn(2)	2.773(3)	Mn(1)−O(1″)	1.936(9)
Fe(3)−Mn(1′)	3.465(3)	Mn(1)−O(2)	1.878(9)
Fe(3)−Mn(1)	3.478(3)	Mn(1)−O(3)	1.852(9)
Fe(3)−Mn(2)	3.357(3)	Mn(1)−O(4)	1.934(9)
Fe(3)−Mn(2′)	3.446(3)	Mn(2)−O(2)	1.890(9)
Fe(3)−O(2)	1.937(9)	Mn(2)−O(3)	1.887(9)
Fe(3)−O(3′)	1.925(9)	Mn(2)−O(5)	2.226(10)
Fe(3)−O(7)	2.037(10)	Mn(2)−O(6)	2.231(11)
Fe(3)−O(9)	2.025(10)	Mn(2)−O(8)	1.953(10)
Fe(3)−O(11)	2.036(10)	Mn(2)−O(10)	1.953(11)
Fe(3)−O(12)	2.097(10)		

(b) Angles

O(2)−Fe(3)−O(3′)	92.8(4)	Fe(3″)−O(3)−Mn(1)	133.2(5)
O(2)−Fe(3)−O(7)	95.5(4)	Fe(3)2−O(3)−Mn(2)	129.4(5)
O(2)−Fe(3)−O(9)	176.3(4)	Mn(1)−O(3)−Mn(2)	95.7(4)
O(2)−Fe(3)−O(11)	93.2(4)	O(1″)−Mn(1)−O(4)	92.6(4)
O(2)−Fe(3)−O(12)	91.5(4)	O(1′)−Mn(1)−O(4)	91.6(4)
O(3′)−Fe(3)−O(7)	93.2(4)	O(1)−Mn(1)−O(4)	174.7(4)
O(3′)−Fe(3)−O(9)	89.7(4)	O(2)−Mn(1)−O(3)	84.6(4)
O(3′)−Fe(3)−O(11)	173.6(4)	O(2)−Mn(1)−O(4)	92.3(4)
O(3)−Fe(3)−O(12)	94.3(4)	O(3)−Mn(1)−O(4)	93.2(4)
O(7)−Fe(3)−O(9)	87.0(4)	O(2)−Mn(2)−O(3)	83.3(4)
O(7)−Fe(3)−O(11)	88.5(4)	O(2)−Mn(2)−O(5)	84.1(4)
O(7)−Fe(3)−O(12)	169.5(5)	O(2)−Mn(2)−O(6)	90.5(4)
O(9)−Fe(3)−O(11)	84.1(4)	O(2)−Mn(2)−O(8)	177.6(4)
O(9)−Fe(3)−O(12)	85.7(4)	O(2)−Mn(2)−O(10)	96.2(4)
O(11)−Fe(3)−O(12)	83.3(4)	O(3)−Mn(2)−O(5)	87.6(4)
O(1)−Mn(1)−O(1″)	83.7(4)	O(3)−Mn(2)−O(6)	91.2(4)
O(1)−Mn(1)−O(1′)	84.1(4)	O(3)−Mn(2)−O(8)	94.5(4)
O(1′)−Mn(1)−O(1″)	80.8(4)	O(3)−Mn(2)−O(10)	175.8(4)
O(1)−Mn(1)−O(2)	91.4(4)	O(5)−Mn(2)−O(8)	94.8(4)
O(1′)−Mn(1)−O(2)	98.5(4)	O(5)−Mn(2)−O(8)	94.8(4)
O(1)−Mn(1)−O(3)	91.0(4)	O(5)−Mn(2)−O(10)	87.9(4)
O(1″)−Mn(1)−O(3)	95.6(4)	O(6)−Mn(2)−O(8)	90.5(4)
O(1′)−Mn(1)−O(3)	174.2(4)	O(6)−Mn(2)−O(10)	93.2(5)
Mn(1′)−O(1)−Mn(1″)	99.1(4)	O(8)−Mn(2)−O(10)	85.9(4)
Fe(3)−O(2)−Mn(1)	131.4(5)	Mn(1)−O(1)−Mn(1″)	95.6(4)
Fe(3)−O(2)−Mn(2)	122.5(5)	Mn(1)−O(1)−Mn(1′)	95.2(4)
Mn(1)−O(2)−Mn(2)	94.7(4)		

[a] Only those involving metal atoms; a full listing is available as supplementary material.

Table 4. Comparison of Selected Structural Parameters for Complexes **1** and **3**[e]

param[a,b]	complex **1**[c]	complex **3**[c]
$Mn^{IV}-O_c$(eq)	1.912(8)	1.930(9)
$Mn^{IV}-O_c$(ax)	1.901(8)[d]	1.883(10)[d]
$Mn^{IV}-O_r$	1.869(7)	1.865(9)
$Mn^{III}-O_r$	1.886(7)	1.889(9)
$Mn^{IV}-O_c$	1.912(8)[d]	1.934(9)[d]
$Fe^{III}-O_r$	1.897(8)	1.931(9)
$Fe^{III}-O_w$	2.178(9)[d]	2.097(10)[d]
$Fe^{III}-O_a$(ax)	2.132(8)[d]	2.037(10)[d]
$Fe^{III}-O_s$(eq)	1.994(8)	2.030(10)
$Mn^{III}-O_a$(ax)	2.218(10)	2.229(11)
$Mn^{III}O_1$(eq)	1.933(8)	1.953(11)
$Mn^{IV}\cdots Mn^{IV}$(eq)	2.943(3)	2.938(4)[d]
$Mn^{IV}\cdots Mn^{IV}$(ax)	2.820(3)	2.820(4)[d]
$Mn^{IV}\cdots Mn^{III}$	2.767(3)	2.773(3)[d]
$Mn^{IV}\cdots Fe^{III}$	3.451(3)	3.472(3)
$Fe^{III}\cdots Mn^{III}$	3.371(3)	3.401(3)

[a] Averaged using the virtual D_{2d} symmetry of the $[Mn_{12}O_{12}$ core]. [b] For complex **1**, replace Fe^{III} with Mn^{III}. [c] Numbers in parentheses are the greatest esd's for a single value. [d] Single value. [e] O_c = central cubane oxygens, O_r = outer ring oxygens, O_a = acetate oxygen, and O_w = water oxygens.

(13) Schmitt, E. A.; Hendrickson, D. N., unpublished results.
(14) Cohn, M. J.; Timken, M. D.; Hendrickson, D. N. *J. Am. Chem. Soc.* **1984**, *106*, 6683.
(15) Chrisman, B. L.; Tumolillo, T. A. *Comput. Phys. Commun.* **1971**, *2*, 322.

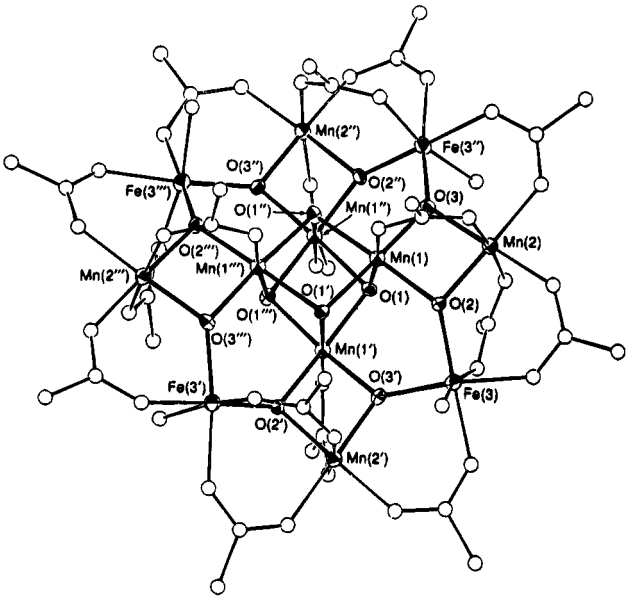

Figure 1. ORTEP representation of $[Mn_8Fe_4O_{12}(O_2CMe)_{16}(H_2O)_4]\cdot 2MeCO_2H\cdot 4H_2O$ at the 50% probability level. The acetic acid and water molecules which are present as solvate molecules are not shown.

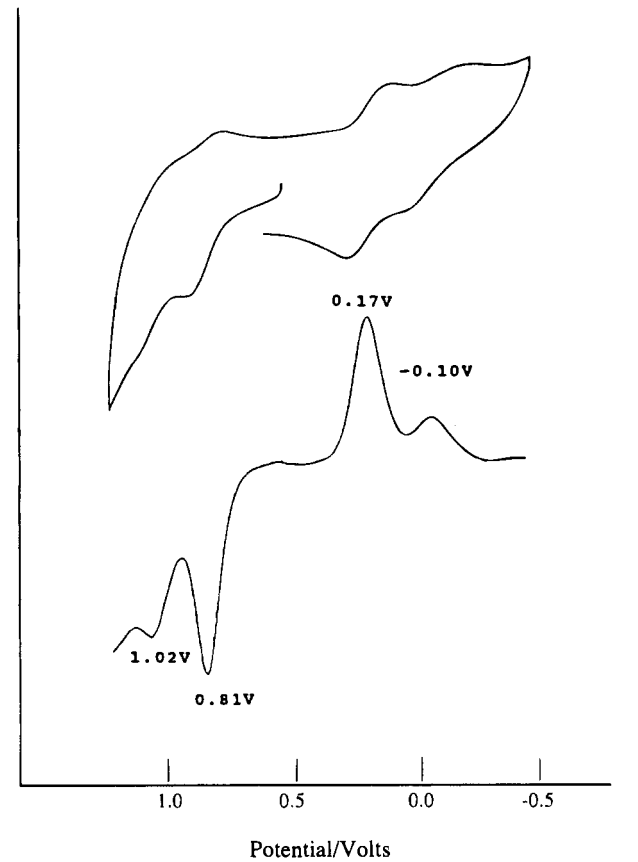

Figure 2. Cyclic voltammogram (top) and differential pulse voltammogram (bottom) of complex $3\cdot 2MeCO_2H\cdot 4H_2O$ in MeCN. The indicated potentials are given versus the ferrocene/ferrocenium couple measured under the same conditions.

^{57}Fe Mössbauer spectra were run at 100 and 300 K for polycrystalline sample (c) of $3\cdot 2MeCO_2H\cdot 4H_2O$, see Figure 3. DC magnetic susceptibility data were also collected at 10.0 kG for this same sample in the 5.0−300.0 K range, see Figure 4. The crystallites were fixed in parafilm to prevent torquing in an external magnetic field. Reduced magnetization data, $M/N\mu_B$ where M is the magnetization and N is Avogadro's number, were also run for the same sample restrained in parafilm at fields

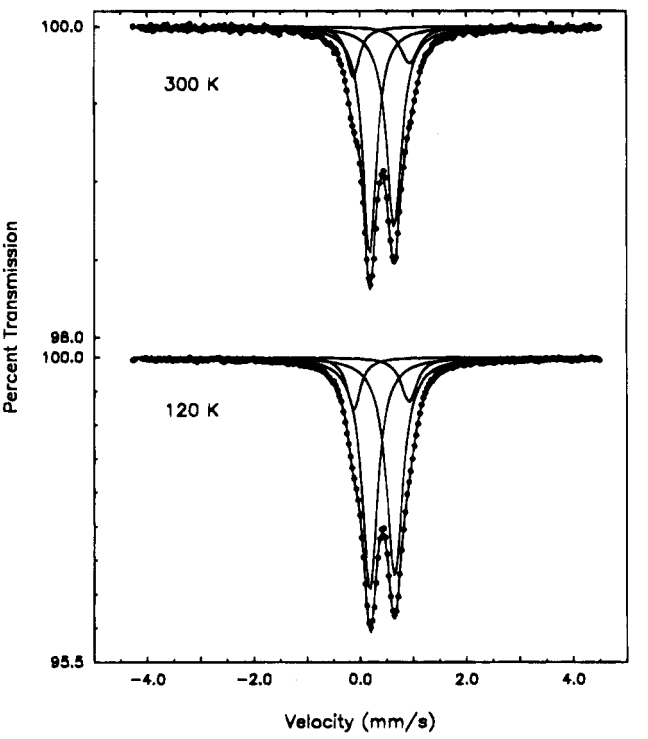

Figure 3. ^{57}Fe Mössbauer spectra at 120 and 300 K for a polycrystalline sample of $[Mn_8Fe_4O_{12}(O_2CMe)_{16}(H_2O)_4]\cdot 2MeCO_2H\cdot 4H_2O$. The solid lines represent a least-squares fit of the spectra to Lorentzian line shapes assuming there are two quadrupole-split doublets.

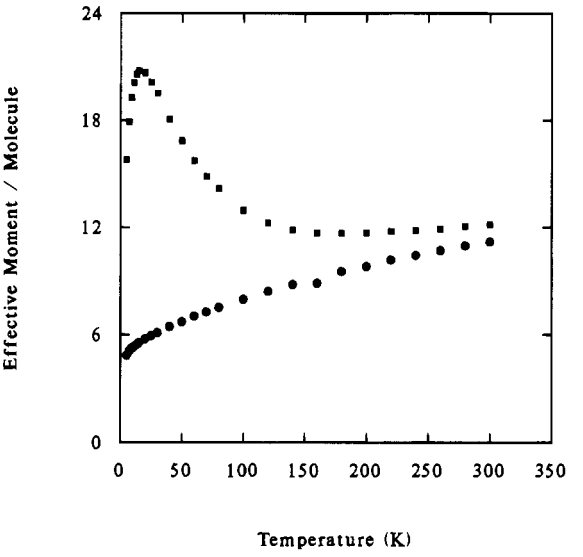

Figure 4. Plots of effective magnetic moment per molecule versus temperature for parafilm-embedded polycrystalline samples of (●) $[Mn_8Fe_4O_{12}(O_2CMe)_{16}(H_2O)_4]\cdot 2MeCO_2H\cdot 4H_2O$ and (■) $[Mn_{12}O_{12}(O_2CMe)_{16}(H_2O)_4]\cdot 2MeCO_2H\cdot 4H_2O$. The measurements were carried out in an external magnetic field of 10.0 kG.

of 0.50−50.0 kG and in the range of ca. 2.0−30.0 K. In Figures 5 and 6 are shown plots of $M/N\mu_B$ versus H/T.

Discussion

Compound Preparation. It was our hope, at the outset of these studies, that the incorporation of Fe^{III} into the $[Mn_{12}O_{12}]$ core would prove to be straightforward and thus allow a family of $[Fe_xMn_{12-x}]$ (x = various) complexes to be accessed with obvious benefits to the magnetochemical goals of this work. This, however, did not turn out to be the case.

It should first be pointed out that the procedure employed for the preparation of complex **1** involves a comproportionation

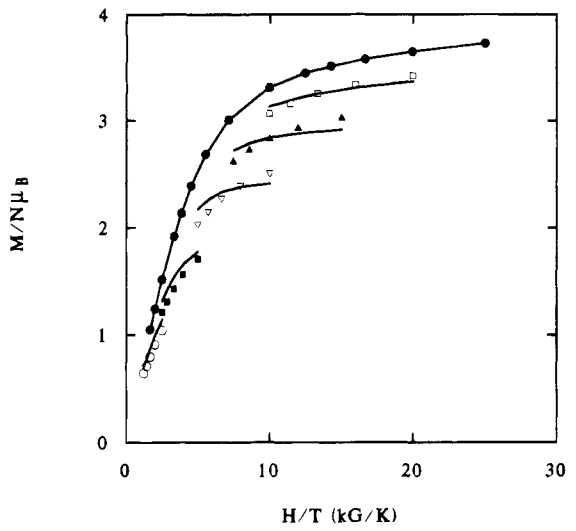

Figure 5. Plots of reduced magnetization, $M/N\mu_B$ where M is magnetization, N is Avogadro's number and μ_B is the Bohr magneton, versus H/T (magnetic field divided by absolute temperature) for a parafilm-embedded polycrystalline sample of $[Mn_8Fe_4O_{12}(O_2CMe)_{16}(H_2O)_4]\cdot 2MeCO_2H\cdot 4H_2O$. Data were collected at magnetic fields of: (●) 50.0 kG; (□) 40.0 kG; (▲) 30.0 kG; (▽) 20.0 kG; (■) 10.0 kG; and (○) 5.00 kG.

reaction between $Mn(O_2CMe)_2\cdot 4H_2O$ and $KMnO_4$ in 60% aqueous acetic acid in a ratio appropriate for the +3.33 average Mn oxidation level in the product (eq 1). It is not obvious from

$$16.3Mn^{2+} + 6.4Mn^{7+} \rightarrow 22.7Mn^{3.4+} \quad (1)$$

this reaction system and eq 1 how, and to what extent it might be possible to incorporate Fe^{III} ions into the product. Since an Fe analogue of $KMnO_4$ is not readily available, the chosen strategy was to replace some $Mn(O_2CMe)_2\cdot 4H_2O$ with $Fe(O_2CMe)_2$. Initial experiments employed equimolar amounts of the two M^{2+} reagents (eq 2), as this would give, very approximately,

$$8.15Mn^{2+} + 8.15Fe^{2+} + 6.4Mn^{7+} \rightarrow 8.15Fe^{3+} + 14.55Mn^{3.6+} \quad (2)$$

the Mn:Fe ratio and oxidation levels appropriate for a possible $[Mn_8Fe_4O_{12}(O_2CMe)_{16}(H_2O)_4]$ product, assuming the presence of $Fe(O_2CMe)_2$ in the reaction mixture would indeed lead to incorporation of Fe but *without* resulting in the formation of a totally different structural type. We were subsequently pleased to see that the product from this reaction exhibited the characteristic IR spectrum of $[M_{12}O_{12}]$ species, but elemental analysis indicated the Fe content to be only approximately 2.5 per 12 metal ions. At this point, an investigation was initiated of the influence of the Fe^{II}:Mn^{II}:Mn^{VII} ratio on the product and its Fe content. Various ratios were explored, of which we mention only the ones investigated the most. Further investigation of the ratio of eq 2 showed that a low Fe content was reproducibly obtained, but nicely crystalline materials could not be obtained and analytical data suggested that the overall purity of the M_{12} product was less-than-acceptable.

In an attempt to increase the Fe content and obtain better-looking material, the Fe:Mn ratio was increased (eq 3), removing

$$16.3Fe^{2+} + 6.4Mn^{7+} \rightarrow 16.3Fe^{3+} + 6.4Mn^{4.5+} \quad (3)$$

$Mn(OAc)_2\cdot 4H_2O$ from the reaction. As indicated in eq 3, the Fe is in excess and the "average" Mn oxidation state in the reaction is high (~4.5+); nevertheless, this ratio produces highly crystalline product that has a reproducible analysis consistent (*vide infra*) with the formulation $[Mn_8Fe_4O_{12}(O_2CMe)_{16}(H_2O)_4]$ (**3**) as supported by subsequent crystallographic characterization. Since the excess of Fe in eq 3 still yielded an $[Mn_8Fe_4]$ product, the amount of Fe^{II} was increased even further by halving the $KMnO_4$ amount, *i.e.*, a Fe^{2+}:Mn^{7+} = 16.3:3.2 ratio. This high ratio led to solids that appeared by IR to contain not only M_{12} compounds but also additional products, possibly $[Fe_3O(O_2CMe)_6]^+$-containing species; elemental analyses gave ratios of Fe:Mn = ~9:3.

Although more than one Fe:Mn ratio gives products that are encouraging *vis-a-vis* either (i) reproducible Fe content, (ii) spectroscopic indications of purity and/or (iii) crystallinity, only the reaction ratio of eq 3 gives a product that is acceptable by all three criteria, and only this product has therefore been subjected to detailed study. Further work is required if the same level of characterization is to be achieved for other Fe_xMn_{12-x} species.

It should be added that even the best preparation, *i.e.*, complex **3**, does not analyze for integral values of Fe:Mn content. The analyses in the Experimental Section of samples from different preparations yield values in the range 4.23−4.51 Fe:7.77−7.49 Mn. Given the inherent inaccuracies in metal analyses, these ranges are satisfyingly narrow, and the Fe:Mn ratios in these samples are probably the same within experimental error. It is clear, however, that the Fe content is definitely greater than 4 Fe per molecule. This is supported by the Mössbauer studies (*vide infra*). The Fe analytical figures represent an Fe content per molecule approximately 6−13% greater than for the $[Mn_8Fe_4]$ formulation. There is no indication in the IR spectrum or electrochemical studies of an Fe impurity, and our belief is that the extra Fe arises from some Mn_8Fe_4 molecules having additional Fe^{III} ions at the Mn^{III} sites. No single species need be responsible for this, *i.e.*, $[Mn_{8-y}Fe_{4+y}]$ (y = 1, 2, 3, 4) could, in principle, all be present in small amounts.

Description of Structure. Complex **3**$\cdot 2MeCO_2H\cdot 4H_2O$ crystallizes in the tetragonal space group $I\bar{4}$ (isomorphous with **1**$\cdot 2MeCO_2H\cdot 4H_2O$) and contains discrete $[Mn_8Fe_4O_{12}(O_2CMe)_{16}(H_2O)_4]$ units with imposed S_4 symmetry. Atomic coordinates are given in Table 2. Selected bond distances and angles are listed in Table 3; a complete listing is available in the supplementary material, where a fully-labeled figure and stereoview are also provided. The structure, shown in Figure 1, is extremely similar to that of **1** and **2**. There is a central $[Mn_4O_4]^{8+}$ cubane held within a nonplanar ring of eight Mn/Fe atoms by eight μ_3-O^{2-} ions. Peripheral ligation is by sixteen bridging $MeCO_2^-$ and four terminal H_2O groups.

There was no reason to assume that the Fe^{III} positions would be ordered, but close inspection of the structural parameters reveals that the Fe^{III} ions are indeed localized at the four symmetry-related positions indicated in Figure 1. One would not normally expect to distinguish by X-ray diffraction techniques the identities of metals with similar atomic numbers except that, in this case, high-spin Mn^{III} (d^4) in near-octahedral symmetry exhibits a Jahn−Teller (JT) distortion, whereas high-spin Fe^{III} (d^5) does not. Thus, Mn(2) shows clear evidence of JT axial elongation, with axial Mn^{III}−acetate bond lengths (average 2.229 Å) significantly longer than equatorial values (average 1.953 Å). In contrast, the Fe^{III}−acetate bond lengths are all identical [2.037(10) *vs* 2.030(10) Å]. Further support for localized Fe^{III} atoms is provided by comparison of **3** with **1**. Selected structural parameters are compared in Table 4. Here can be seen the near-congruency of the two compounds *except* at the Fe(3)/Mn(3) position. In complex **3**, there is no difference in Fe^{III}−acetate bond lengths, as mentioned above; in contrast, in complex **1**, the Mn^{III} ion at this site shows a clear JT axial

elongation with axial Mn^{III}—acetate lengths [2.132(8) Å] being significantly longer than equatorial values [1.994(8) Å average]. We therefore conclude that the structural parameters of **3** indicate Fe^{III} ions at one site and Mn^{III} ions at the other. It should be noted that the two sites are symmetry-inequivalent, perhaps providing the rationale for the Fe^{III} preference for one site over the other. Note also that there is no evidence from the structural parameters or thermal ellipsoids for partial occupation of the Mn^{III} sites by the "extra" Fe^{III} mentioned earlier; given the small amounts of this additional Fe, as indicated by the elemental analyses, this is not surprising.

^{57}Fe Mössbauer Spectroscopy. In Figure 3 are shown the 120 and 300 K spectra of polycrystalline sample c of $3{\cdot}2MeCO_2H{\cdot}4H_2O$. Even without fitting the 300 K spectrum, it is clear that there are two quadrupole-split doublets in the spectrum. Least-squares fitting the 300 K spectrum with Lorentzian line shapes indicates that there are two doublets present, one with a quadrupole splitting (ΔE_Q) of 0.459(4) mm/s and an isomer shift (δ) versus iron foil of 0.416(2) mm/s. This doublet was found to make up 82.6% of the spectral area. The other doublet (shoulders) was fit with ΔE_Q = 1.061(2) mm/s and δ = 0.405(1) mm/s and corresponds to 17.4% of the area. It is clear from these isomer shifts that both are high-spin Fe^{III} ions. The more intense doublet corresponds to the four Fe^{III} ions identified in the X-ray structure. The relatively small ΔE_Q value agrees with a nearly octahedral $Fe^{III}O_6$ site. The weaker doublet likely corresponds to the "excess" Fe^{III}. These Fe^{III} ions are believed to be randomly distributed throughout the Mn^{III} sites. The larger value of ΔE_Q = 1.061(2) mm/s is consistent with this, for these Fe^{III} ions are probably forced to take Mn^{III}-like coordination sites, where there is an appreciable Jahn–Teller distortion.

The 120 K spectrum in Figure 3 was also least-squares fit to two doublets. The more intense doublet corresponds to 83.4% of the area and has ΔE_Q = 0.465(3) mm/s and δ = 0.4185(12) mm/s. The weaker doublet with 16.6% of area was fit with ΔE_Q = 1.038(10) and δ = 0.404(5) mm/s. Thus, Mössbauer spectroscopy indicates that there is ~17% of excess Fe^{III}, whereas the chemical analysis for this same sample indicated ~9% of excess Fe^{III}. These two assessments are probably within experimental error in view of the errors in metal analyses and the fact that the recoilless fractions of the two different Fe^{III} sites may differ because the complexes containing excess Fe^{III} could well be in defect sites in the microcrystals.

Electrochemical Studies. Complex **3** has been investigated by cyclic voltammetry (CV) and differential pulse voltammetry (DPV) to complement similar studies performed previously on complexes **1** and **2**.[10] In Figure 2 are displayed the CV and DPV traces for complex **3** in MeCN; they are very similar to those for **1** and **2**. There is a reversible oxidation at 0.81 V (*vs* ferrocene) and a reversible reduction at 0.17 V. In addition, there is a second irreversible reduction at −0.10 V. Complex **1** in MeCN displays the same three features at almost identical potentials, 0.80, 0.19 and −0.07 V. In addition, **1** displays a third irreversible reduction at −0.35 V; such a feature is not clearly seen for **3**. Conversely, however, complex **3** displays a second, irreversible oxidation at 1.02 V, a feature not obvious in the trace for **1**.

Overall, it is clear that incorporation of $4Fe^{III}$ ions into complex **1** has had only minimal effect on the electrochemical properties. The two most important processes for **1**, the one-electron reversible oxidation and reduction, are both also observed for **3**, and at essentially identical potentials. The latter point is noteworthy: considering first the oxidation, electron loss is presumably from an outer M^{III} ion, and since Mn^{IV} is much more accessible than Fe^{IV}, it is reasonable to conclude that the oxidation is occurring at a Mn^{III} ion in **3**. Considering now the reduction, we have elsewhere shown that the one-electron reduced species can be chemically generated by reduction with I^- and can be isolated as a NR_4^+ or PPh_4^+ salt.[12] More recently, the crystal structure of (PPh_4) $[Mn_{12}O_{12}(O_2CEt)_{16}(H_2O)_4]$ has been obtained[16] and the site of reduction has been identified as a Mn^{III} ion, *i.e.*, the complex is a trapped-valence (Mn^{II}, $7Mn^{III}$, $4Mn^{IV}$) complex. Given the similarity between the first reduction potentials of **1** and **3**, we conclude that the reduction is occurring at a Mn^{III} ion in both complexes, *i.e.*, it does not involve the Fe^{III} ions in **3**. Attempts are currently in progress to generate and structurally characterize the reduced form of complex **3**, or a carboxylate-substituted version, to assess this point further. Attempts are also in progress to isolate the oxidized version of **1**, **2** or **3**.

Magnetic Susceptibility. A plot of effective magnetic moment (μ_{eff}) per molecule versus temperature is shown in Figure 4 for polycrystalline sample c of $3{\cdot}2MeCO_2H{\cdot}4H_2O$ embedded in parafilm and in an external field of 10.0 kG. At 300.0 K, μ_{eff}/molecule is 11.18 μ_B and upon decreasing the temperature decreases gradually to 4.85 μ_B at 5.00 K. In Figure 4 a plot of μ_{eff}/molecule for $1{\cdot}2MeCO_2H{\cdot}4H_2O$ in a 10.0 kG field is also shown. As reported[10-12] previously, the magnetochemical behavior for this $Mn^{IV}_4Mn^{III}_8$ complex is quite different than that for the $Mn^{IV}_4Mn^{III}_4Fe^{III}_4$ complex **3**. Complex $1{\cdot}2MeCO_2H{\cdot}4H_2O$ has a μ_{eff}/molecule value of 12.17 μ_B at 300.0 K, which with decreasing temperature increases to a maximum of 20.79 μ_B at 15.0 K, whereupon there is a decrease to 15.79 μ_B at 5.00 K. Thus, the replacement of four Mn^{III} by four Fe^{III} ions has dramatically affected the magnetochemistry of this dodecanuclear complex.

If there were no magnetic exchange interactions present in a $Fe^{III}_4Mn^{IV}_4Mn^{III}_4$ complex, the spin-only effective magnetic moment with g = 2.0 should be 17.20 μ_B/molecule. For a $Mn^{IV}_4Mn^{III}_8$ complex this spin-only value is expected to be 15.87 μ_B/molecule. It is clear from the values of μ_{eff}/molecule measured for complexes **1** and **3** at 300 K that there are in both complexes appreciable exchange interactions present. In fact, the exchange interactions in the $Fe^{III}_4Mn^{IV}_4Mn^{III}_4$ complex **3** are greater than those in complex **1**, for the μ_{eff}/molecule for complex **3** at 300 K is much lower than its expected spin-only value compared to the $Mn^{IV}_4Mn^{III}_8$ complex **1**. Owing to the topology of complex **3** it is not possible to use the Kambe[17] operator replacement technique to simplify the Hamiltonian equation for such a dodecanuclear complex. Previous studies[10] of complex $1{\cdot}2MeCO_2H{\cdot}4H_2O$ have established that this $Mn^{IV}_4Mn^{III}_8$ complex has a S = 10 ground state. It is clear from Figure 4 that complex $3{\cdot}2MeCO_2H{\cdot}4H_2O$ has a ground state with a total spin that is considerably less than S = 10.

One of the best ways to determine the spin of the ground state of the $Fe^{III}_4Mn^{IV}_4Mn^{III}_4$ complex **3** is to measure the magnetization of a sample as a function of external magnetic field at low temperatures. Magnetization data were run for a parafilm-embedded sample at 50.0 kG in the 2.0–30.0 K range and at fields of 40.0, 30.0, 20.0, 10.0, 5.00, 3.00, 2.00, 1.00, and 0.500 kG in the 2.00–4.00 K range. In Figure 5 is shown a plot of reduced magnetization ($M/N\mu_B$, where M is the magnetization and N is Avogadro's number) versus H/T for all of the data collected in the 5.00–50.0 kG field range. At 50.0 kG and 2.00 K, the value of $M/N\mu_B$ is 3.76. It can be seen that the data sets measured at the different fields in the 5.00–50.0

(16) Tsai, H.-L.; Eppley, H. J.; de Vries, N.; Folting, K.; Christou, G.; Hendrickson, D. N. *J. Chem. Soc., Chem. Commun.* **1994**, 1745.
(17) Kambe, K. *J. Phys. Soc. Jpn.* **1950**, *5*, 48.

kG range do not plateau at the same value. If there is only one state populated at these low temperatures and applied fields, then the nonsuperimposability of the six isofield data sets indicates that the ground state has appreciable zero-field splitting.

The magnetization for such a complex may be calculated by using the basic thermodynamic relation[18] given in eq 4. This

$$M = N\sum_{i=1}^{P}\left(\frac{-\delta E_i}{\delta H}\right)\exp(-E_i/kT)/\sum_{i=1}^{P}\exp(-E_i/kT) \qquad (4)$$

equation reduces to the Brillouin function in the case of no zero-field splitting. In eq 4, $\delta E_i/\delta H$ is the change in the energy of the ith spin state in response to a change in the magnetic field. The energies of the various spin sublevels are obtained by diagonalization of the spin Hamiltonian matrix, including Zeeman interactions and axial zero-field splitting. Thus, in fitting the data it is assumed that there is only one state with total spin S thermally occupied and the spin Hamiltonian matrix is only of dimensions $(2S + 1) \times (2S + 1)$.

The solid lines in Figure 5 represent a least-squares fit of the six isofield data sets obtained in the range of 5.00−50.0 kG. The spin of the ground state was taken as $S = 2$, and the least-squares fitting parameters were found to be $g = 2.18$ and $D = -2.10$ cm^{-1}, with the temperature-independent paramagnetism (TIP) for the complex held fixed at 2400×10^{-6} cgsu. The parameter D characterizes the axial ($D\hat{S}_z^2$) zero-field splitting in the $S = 2$ ground state. Least-squares fitting of the same data assuming the ground state has a spin of either $S = 3$ or $S = 1$ gave very unreasonable values of the g factor. It is possible to conclude that, if complex **3**·2MeCO$_2$H·4H$_2$O has only one state populated in the 2.0−30.0 K and 5.00−50.0 kG range, then this ground state has a spin of $S = 2$. However, complex **3** has 1 389 242 different $S = 2$ spin states! Only one of them is the ground state.

A second analysis of the above magnetization data was carried out. In this case all data obtained in the 5.00−50.0 kG range were used, except that the temperature was restricted to the 2.00−4.00 K range. Least-squares fitting of these data to the spin Hamiltonian for a $S = 2$ state gave g = 2.06 and $D = -1.60$ cm^{-1}. This g value is somewhat more reasonable than the $g = 2.18$ value obtained in the previous fitting. This could indicate that even though there is a $S = 2$ ground state in complex **3** with an applied field of 5.00−50.0 kG, there may be low-lying excited states which are populated as the temperature is increased from 2.00 K to 30.0 K.

Low-field magnetization studies were carried out to further characterize the ground state of complex **3**. Magnetization data were collected at 3.00, 2.00, 1.00 and 0.50 kG in the 2.00−4.00 K range. Figure 6 shows a plot of $M/N\mu_B$ versus H/T for data at these four low fields and also at 5.00 and 10.0 kG. All of the data shown in Figure 6 were least-squares fit to the spin Hamiltonian for a $S = 2$ state to give the parameters $g = 2.05$ and $D = -1.80$ cm^{-1}. The solid lines in Figure 6 show that this fit is good. These parameters are essentially the same parameters obtained in fitting the higher field data measured in the 2.00−4.00 K range. Thus, even at low fields complex **3** seems to have a $S = 2$ ground state. However, because there is some amount of extra Fe content beyond Fe_4Mn_8, the g and D values obtained in this fitting procedure are probably not well determined.

Spin of the Ground State. The $Mn^{IV}_4Mn^{III}_8$ complex **1** and $Mn^{IV}_4Mn^{III}_4Fe^{III}_4$ complex **3** are isostructural. The former has

(18) Vermaas, A.; Groenveld, W. L. *Chem. Phys. Lett.* **1984**, *27*, 583.

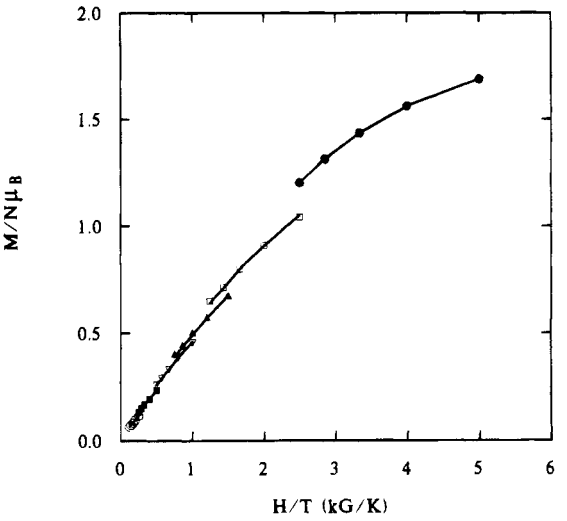

Figure 6. Plots of reduced magnetization, $M/N\mu_B$, versus H/T for a parafilm-embedded polycrystalline sample of $[Mn_8Fe_4O_{12}(O_2CMe)_{16}(H_2O)_4]$·2MeCO$_2$H·4H$_2$O. Data were collected at magnetic fields of: (●) 10.0 kG; (□) 5.00 kG; (▲) 3.00 kG; (▽) 2.00 kG; (■) 1.00 kG; and (○) 0.500 kG.

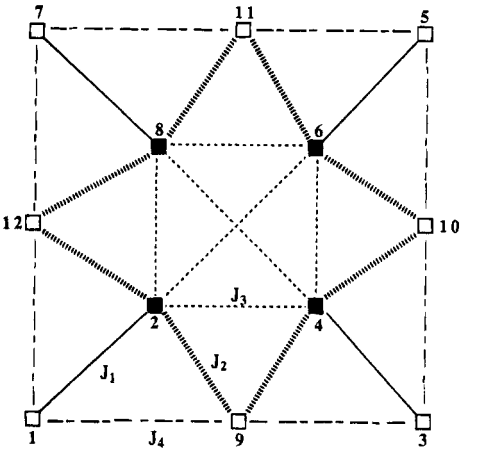

Figure 7. Schematic drawing representing the various pairwise magnetic exchange interactions in the $[Mn_8Fe_4O_{12}(O_2CMe)_{16}(H_2O)_4]$ and $[Mn_{12}O_{12}(O_2CR)_{16}(H_2O)_4]$ (R = Me, Ph) complexes.

a $S = 10$ ground state, whereas the latter has a $S = 2$ ground state. It is not obvious why the replacement of half of the Mn^{III} ions by four Fe^{III} ions leads to such a dramatic change in the spin of the ground state. In Figure 7 is given a schematic drawing showing the various pairwise magnetic exchange interactions in such a dodecanuclear complex. In both complexes the atoms numbered 2, 4, 6, and 8 are four Mn^{IV} ions ($S = {}^3/_2$) which form the cubane core. For complex **1** all of the other metal ions are Mn^{III} ions ($S = 2$). For complex **3** the ions numbered 9, 10, 11, and 12 are Fe^{III} ions ($S = {}^5/_2$) and atoms 1, 3, 5, and 7 are Mn^{III} ions ($S = 2$).

In our previous theoretical calculations of spin-state orderings in the acetate and benzoate $Mn^{IV}_4Mn^{III}_8$ complexes, it was recognized that the J_4-type Mn^{III}···Mn^{III} interactions are known to be weak, either ferromagnetic or antiferromagnetic with $|J_4| \leq 30$ cm^{-1}. Furthermore, the J_1-type Mn^{IV}···Mn^{III} interaction is antiferromagnetic (approximately -150 cm^{-1}) and larger than all the others in this complex. Thus, it was concluded that the four

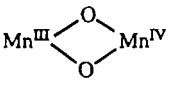

J_1-type moieties (represented as $Mn^{III}(O_2)Mn^{IV}$) are spin paired to give $S = {}^1/_2$ units. As a consequence a $Mn^{IV}_4Mn^{III}_8$ complex can be viewed as four $Mn^{III}(O_2)Mn^{IV}$ $S = {}^1/_2$ units interacting with four $S = 2$ Mn^{III} ions (atom 9, 10, 11 and 12). With these approximations the states for the $Mn^{IV}_4Mn^{III}_8$ complex range from a spin of 0 to 10, and the largest block in the spin Hamiltonian matrix is that for the $S = 3$ states which give a 248 × 248 block. We showed in our previous paper[10] that if $J_4 = 0$, J_1 is taken as large and negative, and $J_2 = J_3 \simeq -60$ cm^{-1}, then the spin of the ground state is in the range of $S = 10$ or $S = 9$. Minor variations of J_2 and J_3 alter the spin of the ground state. The calculations also showed that under the above assumptions there would be low-lying (energy less than 5 cm^{-1}) excited spin states near to the ground state.

Relative to the $Mn^{IV}_4Mn^{III}_8$ complexes **1** and **2**, the magnitudes of the J_2 and J_4 interactions in the $Mn^{IV}_4Mn^{III}_4Fe^{III}_4$ complex **3** are expected to be considerably different. The J_3 interaction is the same and from our previous calculations[10] is of the order $J_3 \simeq -60$ cm^{-1}. The value for the $Mn^{III}(O_2)Mn^{IV}$ J_1-type interaction would also be the same as in complex **1**. From the several examples of $Mn^{III}(O_2)Mn^{IV}$ dinuclear complexes in the literature[19] we would anticipate that $J_1 \simeq -150$ cm^{-1}. The very recent work of Hotzelmann *et al.*[20] dealing with magnetic exchange interactions in asymmetric heterodinuclear complexes containing the (μ-oxo)bis(μ-acetato)dimetal core gives insight about the values of J_2 and J_4 for $Mn^{IV}_4Mn^{III}_4Fe^{III}_4$ complex **3**. Data were presented[20] for two complexes which have a $[Mn^{III}(\mu\text{-O})(\mu\text{-}CH_3CO_2)_2Fe^{III}]^{2+}$ core. Exchange parameters of $J = -63$ and -68 cm^{-1} ($\hat{H} = -2J_{ij}\hat{S}_i\hat{S}_j$ Hamiltonian) were determined for these two complexes. In complex **3** the J_4 interaction occurs between a Mn^{III} ion and a Fe^{III} ion bridged by one μ-oxo and two μ-$CH_3CO_2^-$ bridges. Thus, this interaction may be of the magnitude of $J_4 \simeq -65$ cm^{-1}. Finally, the J_2 interaction in complex **3** involves a Fe^{III}-OMn^{IV} pair. This is isostructural and isoelectronic to $Fe^{III}OCr^{III}$, which Hotzelmann *et al.*[20] reported for one complex to have $J = -138$ cm^{-1}.

In summary, for $Mn^{IV}_4Mn^{III}_4Fe^{III}_4$ complex **3** the order of exchange interactions is expected to be $J_1 \simeq -150$ cm^{-1}, $J_2 \simeq -138$ cm^{-1}, $J_4 \simeq -65$ cm^{-1} and $J_3 \simeq -60$ cm^{-1}. If these expectations are correct, then it is clear that there is no simplifying approximation that can be employed to carry out quantitative calculations as we reported[10] for the $Mn^{IV}_4Mn^{III}_8$ complexes. Even with the efficient procedure very recently designed by Gatteschi and Pardi[21] for the calculation of spin-state energy levels in polynuclear complexes, the blocks in the Hamiltonian matrix for complex **3** are too large.

The only recourse is to resort to a qualitative analysis of why the spin of the ground state changes from $S = 10$ for $Mn^{IV}_4Mn^{III}_8$ complex **1** to $S = 2$ for $Mn^{IV}_4Mn^{III}_4Fe^{III}_4$ complex **3**. Some insight can be had by assuming that for complex **3** the J_3-type interactions in the cubane core of complex **3** are negligible. It is then possible to view complex **3** as resulting from fusing together at the wing tips four butterfly complexes, each of which has the following structure

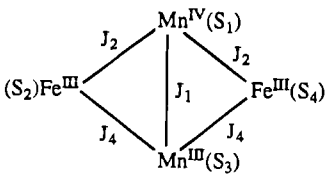

If we make the additional approximation that $J_2 = J_4$, then the Kambe equivalent operator technique can be used to evaluate the energies of the spin states of this butterfly complex. Such a $Mn^{IV}Mn^{III}Fe^{III}_2$ complex has 90 spin states with spin values ranging from $S = {}^1/_2$ to $S = 8.5$. As the ratio of J_2/J_1 is increased from 0 to 1.0 the ground state of the $Mn^{IV}Mn^{III}Fe^{III}_2$ butterfly complex takes on the spin of ${}^9/_2$, ${}^7/_2$, ${}^5/_2$ or ${}^3/_2$. The variation in spin of the ground state of this butterfly complex is a manifestation of spin frustration.[22] Even though all pairwise interactions are antiferromagnetic in a polynuclear complex, certain molecular topologies lead to spin frustration where unpaired electrons on neighboring metal ions cannot spin pair totally because they are also involved in exchange interactions with other metal ions. Ground states with spins intermediate between the minimum and maximum values result.

The spin frustration present in the $Mn^{IV}Mn^{III}Fe^{III}_2$ butterfly complex is likely intermediate between that present in butterfly Fe^{III} and Mn^{III} complexes which have the same $[M_4O_2]^{8+}$ core. The bis(μ_3-oxo) core of these complexes is pictured as follows:

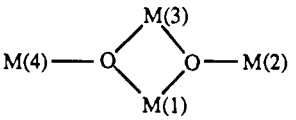

In the case of $[Mn^{III}_4O_2]^{8+}$ complexes[19,23] the body–body antiferromagnetic interaction (J_1) is much larger than the body–wing tip interaction (J_2). The spins on the Mn(1) and Mn(3) ions have the greater tendency to pair up. However, S_{13} (=$S_1 + S_3$) equals 1, not 0 which would be found for total coupling. Each wing-tip Mn^{III} ion [Mn(2) and Mn(4)] interacts with both the Mn(1) and Mn(3) ions. The net result is that the spin alignments of the wing-tip ions are frustrated. For the two $[Mn^{III}_4O_2]^{8+}$ complexes which have been characterized,[19,23] the ground states have a total spin of $S_T = 3$ which arise from $S_{13} = 1$ and $S_{24} = 4$, where $\hat{S}_T = \hat{S}_{13} + \hat{S}_{24}$, $\hat{S}_{13} = \hat{S}_1 + \hat{S}_3$, and $\hat{S}_{24} = \hat{S}_2 + \hat{S}_4$. Even though both types of pairwise exchange interactions are antiferromagnetic, the ground state of these two complexes has 6 unpaired electrons. This results from spin frustration.

Butterfly $[Fe^{III}_4O_2]^{8+}$ complexes have a spin frustration which is quite different than that found in the above $[Mn^{III}_4O_2]^{8+}$ analogs. For the Fe^{III} complexes the strongest antiferromagnetic pairwise interaction occurs between one wing-tip ion and one of the body ions. This leads to a spin frustration of the two body ions Fe(1) and Fe(3). The spins on these two body ions tend to be parallel. For the $[Fe^{III}_4O_2]^{8+}$ complexes studied[24] the result was found to be a ground state with $S_T = 0$. There are, in fact, six spin states of the $[Fe_4O_2]^{8+}$ complex which have

(19) A tabulation of exchange parameters for pairwise interactions of manganese ions in different oxidation states can be found in: Vincent, J. B.; Christmas, C.; Chang, H.-R.; Li, Q.; Boyd, P. D. W.; Huffman, J. C.; Hendrickson, D. N.; Christou, G. *J. Am. Chem. Soc.* **1989**, *111*, 2086.

(20) Hotzelmann, R.; Wieghardt, K.; Flörke, U.; Haupt, H.-J.; Weatherburn, D. C.; Bonvoisin, J.; Blondin, G.; Girerd, J.-J. *J. Am. Chem. Soc.* **1992**, *114*, 1681.

(21) Gatteschi, D.; Pardi, L. *Gazz. Chim. Ital.* **1993**, *123*, 231.

(22) (a) Hendrickson, D. N. Spin Frustration in Polynuclear Complexes. In *Research Frontiers in Magnetochemistry*; O'Connor, C. J., Ed.; World Scientific Publishing Co.: London, 1993, in press. (b) McCusker, J. K.; Schmitt, E. A.; Hendrickson, D. N. In ref 2a, pp 297–319. (c) McCusker, J. K.; Christmas, C. A.; Hagen, P. M.; Chadha, R. K.; Harvey, D. F.; Hendrickson, D. N. *J. Am. Chem. Soc.* **1991**, *113*, 6114. (d) Hendrickson, D. N.; Christou, G.; Schmitt, E. A.; Libby, E.; Baskin, J. S.; Wang, S.; Tsai, H.-L.; Vincent, J. B.; Boyd, P. D. W.; Huffman, J. C.; Folting, K.; Li, Q.; Streib, W. E. *J. Am. Chem. Soc.* **1992**, *114*, 2455.

(23) Libby, E.; McCusker, J. K.; Schmitt, E. A.; Folting, K.; Huffman, J. C.; Hendrickson, D. N.; Christou, G. *Inorg. Chem.* **1991**, *30*, 3486.

(24) (a) McCusker, J. K.; Vincent, J. B.; Schmitt, E. A.; Mino, M. L.; Shin, K.; Coggin, D. K.; Hagen, P. M.; Huffman, J. C.; Christou, G.; Hendrickson, D. N. *J. Am. Chem. Soc.* **1991**, *113*, 3012. (b) Armstrong, W. H.; Roth, M. E.; Lippard, S. J. *J. Am. Chem. Soc.* **1987**, *109*, 6318.

$S_T = 0$. All of the known complexes have $S_{13} = 5$ and $S_{24} = 5$. Thus, the $[Mn^{III}_4O_2]^{8+}$ and $[Fe^{III}_4O_2]^{8+}$ complexes essentially have the two extremes of spin frustration possible for such a butterfly complex.

The spin frustration in the $Mn^{IV}Mn^{III}Fe^{III}_2$ butterflies which are fused together to form $Mn^{IV}_4Mn^{III}_4Fe^{III}_4$ complex **3** is likely intermediate between that found in the $[Mn^{III}_4O_2]^{8+}$ and $[Fe^{III}_4O_2]^{8+}$ complexes. There is not one pairwise antiferromagnetic interaction that dominates. For the $Mn^{IV}Mn^{III}Fe^{III}_2$ complex J_1 and J_2 are probably comparable. This complex can have a ground state with $S_T = {}^9/_2, {}^7/_2, {}^5/_2$ or ${}^3/_2$. These states represent different levels of frustration. In all cases the spins on the two Fe^{III} ions are aligned and $S_{24} = 5$. The value of S_{13} changes in the series ${}^1/_2, {}^3/_2, {}^5/_2$, and ${}^7/_2$ to give the $S_T = {}^9/_2, {}^7/_2, {}^5/_2$, or ${}^3/_2$ ground states respectively. Since J_1 and J_2 are comparable, it is probable such a $Mn^{IV}Mn^{III}Fe^{III}_2$ butterfly complex would have a $S_T = {}^3/_2$ ground state.

Qualitatively we can rationalize the changes in the ground state from $S_T = 10$ for a $Mn^{IV}_4Mn^{III}_8$ complex to $S_T = 2$ for a $Mn^{IV}_4Mn^{III}_4Fe^{III}_4$ complex. The four $Mn^{IV}Mn^{III}_3$ butterflies which are fused together to give complexes **1** and **2** each have strong body-body interactions and the resulting $S_{13} = {}^1/_2$ couples to the spin-aligned Mn^{III} wing-tip ions (*i.e.*, $S_{24} = 4$) to give $S_T = {}^7/_2$ for each butterfly. Fusing the four $Mn^{IV}Mn^{III}_3$ butterflies gives a dodecanuclear complex with $S_T = 10$. On the other hand, the four $Mn^{IV}Mn^{III}Fe^{III}_2$ butterflies each have $S_T = {}^3/_2$ and fusing them together gives $Mn^{IV}_4Mn^{III}_4Fe^{III}_4$ complex **3** with a $S_T = 2$ ground state.

Concluding Comments. The synthesis and X-ray structure of $[Mn_8Fe_4O_{12}(O_2CMe)_{16}(H_2O)_4]\cdot 2MeCO_2H\cdot 4H_2O$ are reported. There is a central $[Mn^{IV}_4O_4]^{8+}$ cubane core held within a nonplanar ring of four Mn^{III} and four Fe^{III} ions by eight μ_3-O^{2-} ions. The Mn^{III} and Fe^{III} ions are in alternating positions. The replacement of four Mn^{III} ions in isostructural $[Mn_{12}O_{12}(O_2CMe)_{16}(H_2O)_4]\cdot 2MeCO_2H\cdot 4H_2O$ by four Fe^{III} ions changes the spin of the ground state of the complex from $S_T = 10$ for $Mn^{IV}_4Mn^{III}_8$ complex **1** to $S_T = 2$ for $Mn^{IV}_4Mn^{III}_4Fe^{III}_4$ complex **3**. This can be qualitatively explained by expected variations in the spin frustration in the butterfly complexes which are fused together to form the dodecanuclear complexes. It would be interesting to prepare other dodecanuclear complexes with different metal ions replacing the Fe^{III} ions.

Acknowledgment. This work was partially supported by NSF grants CHE-9115286 (D.N.H.) and CHE-9311904 (G.C.) and NIH grant HL13652 (D.N.H.).

Supplementary Material Available: Complete listings of crystallographic data, bond lengths and angles, positional and thermal parameters and magnetic susceptibility data and ORTEP diagrams for $[Mn_8Fe_4O_{12}(O_2CMe)_{16}(H_2O)_4]\cdot 2MeCO_2H\cdot 4H_2O$ (15 pages). Ordering information is given on any current masthead page.